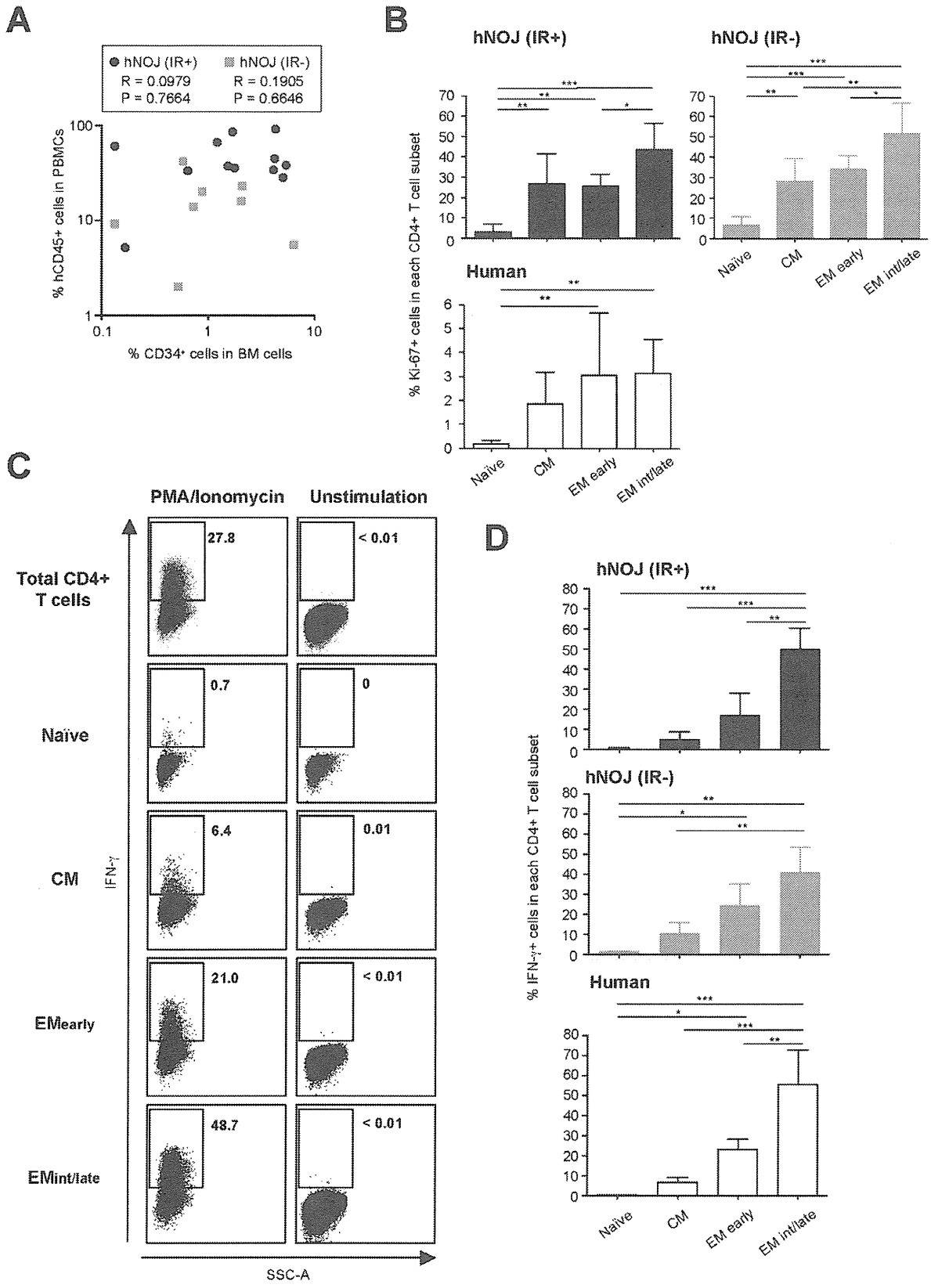

Figure 5. Possible occurrence of HSP of CD4$^+$ T Cells in hNOJ mice. (A) Association between the percentage of hCD45$^+$ cells within the PBMC population and that of CD34$^+$ cells in the BM cells from hNOJ (IR+) and hNOJ (IR−) mice at ≥16 wk post-transplantation ($n=12$ and $n=8$, respectively). Spearman's rank correlation coefficient was used for statistical analysis. (B) Percentage of Ki-67$^+$ cells among naïve, CM, EM_{early}, and $EM_{int/late}$ subsets of splenic CD4$^+$ T cells from hNOJ (IR+) and hNOJ (IR−) mice at ≥16 wk post-transplantation ($n=6$ and $n=6$, respectively) and from human PBMCs ($n=10$). Data are expressed as the mean ± SD. Significant differences ($^*P<0.05$, $^{**}P<0.01$, $^{***}P<0.001$) were determined by Tukey's

multiple comparison test. (C and D) *Ex vivo* IFN-γ production by $CD4^+$ T cells after stimulation with PMA/ionomycin. $CD4^+$ T cells were prepared from the spleens of hNOJ (IR+) and hNOJ (IR−) mice at ≥16 wk post-transplantation or from human PBMCs. (C) Representative flow cytometry profiles showing the proportion of IFN-γ^+ cells within each of the $CD4^+$ T cell subsets from a hNOJ (IR+) mouse at 16 wk post-transplantation. (D) Cumulative data showing the percentage of IFN-γ^+ cells within each of the $CD4^+$ T cell subsets from hNOJ (IR+) and hNOJ (IR−) mice and humans ($n=3$, $n=3$, and $n=4$, respectively). Data are expressed as the mean ± SD. Significant differences ($^*P<0.05$, $^{**}P<0.01$, $^{***}P<0.001$) were determined by Tukey's multiple comparison test.
doi:10.1371/journal.pone.0053495.g005

12 wk post-transplantation, and the difference was statistically significant ($P<0.0001$ and $P<0.0313$). Also, this increase was maintained at about 50−60% beyond 16 wk post-transplantation in hNOJ (IR−) mice (Figure 4A, lower panel). To assess the activation status of $CD4^+$ T cells in other organs, such as the spleen and BM, we next performed an experiment using hNOJ (IR+) mice at 8 wk post-transplantation and hNOJ (IR−) mice at ≥20 wk post-transplantation as representative examples of early- and late-phase, respectively, $CD4^+$ T cell development. We found that the expression of HLA-DR by peripheral blood $CD4^+$ T cells isolated from hNOJ mice was consistent with that by cells isolated from the spleen and BM: lower expression of HLA-DR (7.7% and 17.1% in two hNOJ (IR+) mice) during the early phase (8 wk) post-transplantation, which is also equivalent to that in human PBMCs, and higher expression (68.7−93.8% in four hNOJ (IR−) mice) during the later phase (≥20 wk) post-transplantation (Figure 4B). To address whether HLA-DR expression actually reflects the activation status of reconstituted $CD4^+$ T cells, we examined the expression of other activation markers: CD11a, CD38, and CD150. Figure 4C shows representative flow cytometry profiles obtained using peripheral blood $CD4^+$ T cells isolated from one of four hNOJ (IR+) mice at 16 wk post-transplantation. HLA-DR^+CD4^+ T cells also expressed these markers, confirming the highly activated status of the HLA-DR^+CD4^+ T cells reconstituted in hNOJ mice.

We further investigated whether the activation status of $CD4^+$ T cells was associated with their differentiation stage. When the total percentage of HLA-DR^+ cells within the peripheral blood $CD4^+$ T cell subset populations was examined, we found that the memory $CD4^+$ T cell subsets, particularly the $EM_{int/late}$ subset, made up a significantly higher proportion of this percentage than the naïve subset ($n=4$; two hNOJ (IR+) and two hNOJ (IR−) mice; Figure 4D). The different HLA-DR expression patterns between the $CD4^+$ T cell subsets were similar in human PBMCs ($n=3$), although the expression levels were much lower than those in hNOJ mice (Figure 4D). To further address this differentiation stage-dependent level of HLA-DR expression by $CD4^+$ T cells, we compared the percentage of each $CD4^+$ T cell subset with the percentage of HLA-DR^+ cells within the total $CD4^+$ T cell population using data obtained from peripheral blood samples routinely collected from hNOJ (IR+) and hNOJ (IR−) mice ($n=25$ and $n=21$, respectively) within 25 wk and 28 wk post-transplantation, respectively. We found that the percentage of HLA-DR^+ cells positively correlated with that of the EM_{early} and $EM_{int/late}$ subsets, and inversely correlated with that of the naïve subset, in both hNOJ (IR+) and hNOJ (IR−) mice (Figure 4E). However, there was no significant correlation between the percentage of HLA-DR^+ cells and that of the CM subset in either hNOJ (IR+) or hNOJ (IR−) mice, indicating an intermediate stage at which cells are acquiring the activation phenotype (Figure 4E). Taken together, reconstituted $CD4^+$ T cells in hNOJ mice express a unique phenotype compared with human peripheral blood $CD4^+$ T cells: activated EM subsets predominate with time after transplantation.

Homeostatic Peripheral Expansion of $CD4^+$ T Cells May Occur in hNOJ Mice

When the percentage of $hCD45^+$ leukocytes within the total PBMC population was compared with that of $CD34^+$ cells within the total BM cell population during the later phase (≥16 wk) post-transplantation, no significant correlation was observed in either hNOJ (IR+) or hNOJ (IR−) mice ($n=12$ and $n=8$, respectively) (Figure 5A). These results prompted us to assume that $CD4^+$ T cell proliferation/expansion was predominant in hNOJ mice during the late phase post-transplantation. Therefore, we next examined the expression of a proliferation marker, Ki-67, by reconstituted $CD4^+$ T cells using flow cytometry to assess the proliferative capacity at different differentiation stages. $CD4^+$ T cells were prepared from the spleens of hNOJ (IR+) and hNOJ (IR−) mice during the later phase (≥16 wk) post-transplantation ($n=6$ and $n=6$, respectively). $CD4^+$ T cells isolated from human PBMCs ($n=10$) were used as a control. The results showed that Ki-67^+ cells were present within the memory $CD4^+$ T cell subsets (CM, EM_{early} and $EM_{int/late}$) at higher percentages than within the naïve subset (Figure 5B, upper two panels). A higher percentage of Ki-67^+ cells was also observed in the memory subsets within the human PBMC population than in the naïve subset; however, the levels were much lower than those observed in the hNOJ mice (Figure 5B, lower panel). These results support the notion that increased $CD4^+$ T cell proliferation/expansion occurs in hNOJ mice during the later phase post-transplantation.

HSP of $CD4^+$ T cells involves both slow and rapid proliferation pathways. The slow pathway is IL-7-dependent and results in limited cell activation and differentiation, whereas the latter is T cell receptor (TCR)-dependent and IL-7-independent and results in robust cell activation and differentiation into a memory phenotype with the capacity to produce IFN-γ [25,26]. The term "HSP" is generally used to indicate the former; the latter is often referred to as "spontaneous HSP" [25] or "homeostatic peripheral expansion (HPE)" [26]. It was assumed that HPE-type HSP might occur in hNOJ mice, as described elsewhere [27,28]; therefore, we examined the IFN-γ-producing capacity of $CD4^+$ T cells isolated from the spleens of hNOJ (IR+) and hNOJ (IR−) mice ($n=3$ and $n=3$, respectively) during the later phase (16 and 26 wk, respectively) post-transplantation by stimulating them with or without PMA plus ionomycin. Flow cytometric analysis of intracellular IFN-γ staining showed substantial numbers of IFN-γ-producing cells within the $EM_{int/late}$ subset after PMA/ionomycin stimulation; the data were similar when $CD4^+$ T cells from human PBMCs were used in the experiment ($n=4$) (Figure 5C and 5D). No IFN-γ-producing cells were detectable in any of the $CD4^+$ T cell subsets from hNOJ (IR+) and hNOJ (IR−) mice, or in human PBMCs without PMA/ionomycin stimulation (Figure 5C and data not shown).

Next, we measured the concentrations of cytokines (IL-2, IL-7, and IL-15, all of which are involved in $CD4^+$ T cell proliferation [24,42]), in plasma prepared from peripheral blood samples taken from hNOJ (IR+) and hNOJ (IR−) mice ($n=9$ and $n=13$, respectively) at 12, 16, and (occasionally) 20 wk post-transplantation. However, none of these cytokines were present at detectable levels (limit of detection = <3.2 pg/ml).

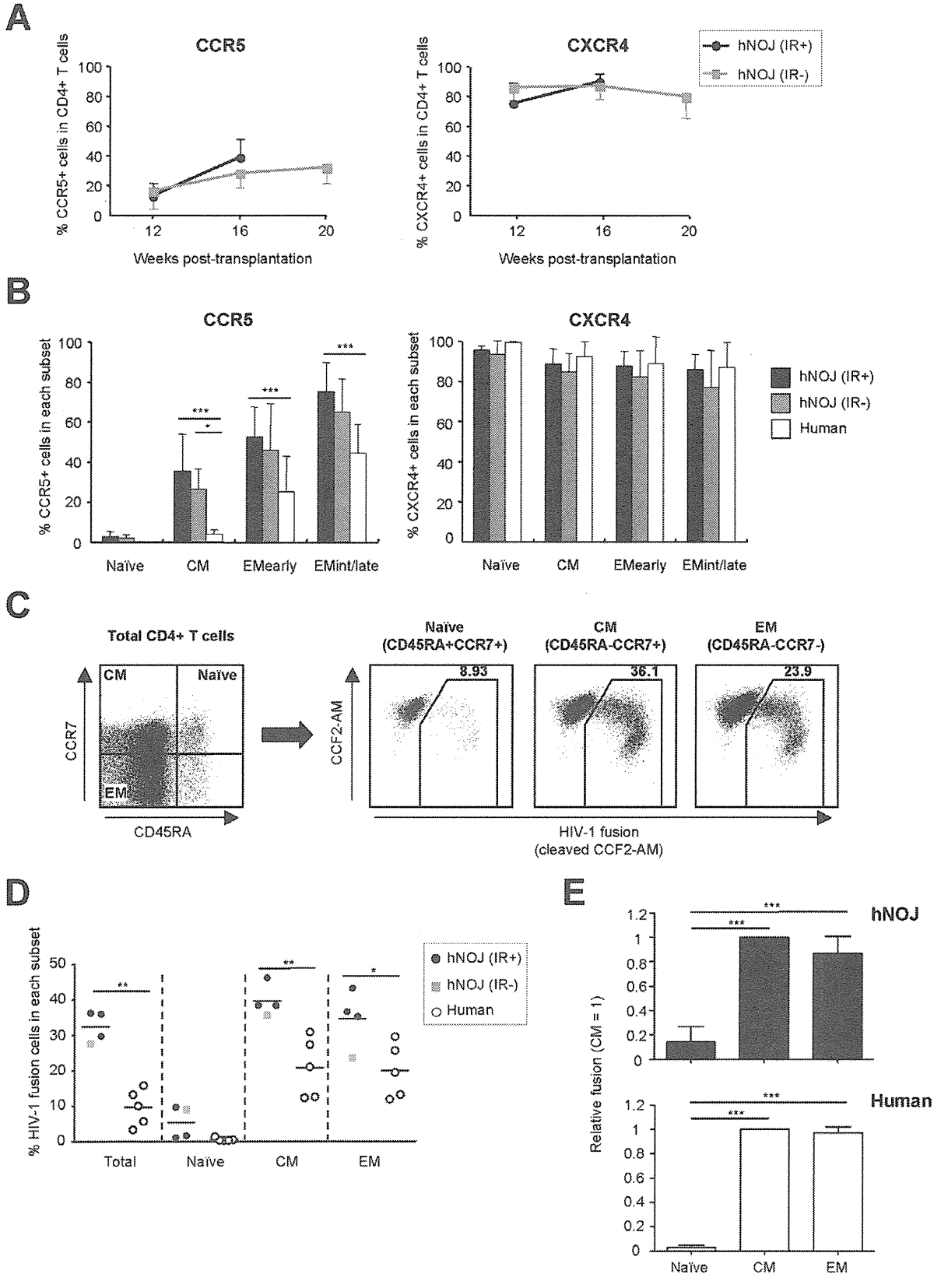

Figure 6. HIV-1 co-receptors, CCR5 and CXCR4, expression profiles and *ex vivo* R5 HIV-1 infectivity of CD4$^+$ T Cells in hNOJ mice. (A) Changes in the percentage of CCR5$^+$ (left) and CXCR4$^+$ (right) cells within the peripheral blood CD4$^+$ T cell population isolated from hNOJ (IR+) and hNOJ (IR−) mice ($n = 18$ and $n = 6$, respectively). Data are expressed as the mean ± SD. (B) Percentage of CCR5$^+$ and CXCR4$^+$ cells within the naïve, CM, EM_{early}, and $EM_{int/late}$ subsets of peripheral blood CD4$^+$ T cells isolated from hNOJ mice at 16 wk post-transplantation ($n = 18$ and $n = 6$, respectively) and from humans ($n = 5$). Data are expressed as the mean ± SD. Significant differences ($^*P<0.05$, $^{***}P<0.001$) were determined by two-

way factorial ANOVA with the Bonferroni multiple comparison test. (C, D, E) Fusion assay using R5 HIV-1 and $CD4^+$ T cells. Splenic $CD4^+$ T cells from hNOJ mice at ≥17 wk post-transplantation ($n=4$; three hNOJ (IR+) mice and one hNOJ (IR−) mouse) or peripheral blood $CD4^+$ T cells from humans ($n=5$) were infected *ex vivo* with HIV-$1_{NL\text{-}AD8\text{-}D\text{-}BlaM\text{-}Vpr}$. (C) Naïve, CM, and EM subsets of $CD4^+$ T cells (gated on $CD3^+CD4^+CD8^-$) were defined as $CD45RA^+CCR7^+$, $CD45RA^-CCR7^+$, and $CD45RA^-CCR7^-$, respectively, by flow cytometry. (D) Percentage of R5 HIV-1 fusion cells within the total $CD4^+$ T cell population and within the naïve, CM, and EM subsets in hNOJ mice and humans. Individual data points are plotted. The black lines represent the mean. Significant differences ($^*P<0.05$, $^{**}P<0.01$) were determined by the unpaired *t* test. (E) Relative ratio of R5 HIV-1 fusion among the naïve, CM, and EM subsets from hNOJ mice and humans. The level of R5 HIV-1 fusion in each of the $CD4^+$ T cell subsets relative to that in the corresponding CM subset. Data are expressed as the mean ± SD. Significant differences ($^{***}P<0.001$) were determined by Tukey's multiple comparison test.
doi:10.1371/journal.pone.0053495.g006

Taken together, these results support the notion that the time-dependent appearance of the activated memory $CD4^+$ T cell subset in hNOJ mice is due to HPE-type HSP.

Expression Profiles of CCR5 and CXCR4 in $CD4^+$ T Cells in hNOJ Mice

The expression profiles of the HIV-1 co-receptors, CCR5 and CXCR4, on $CD4^+$ T cells within the PBMC populations in hNOJ mice and humans were compared by flow cytometry. The percentage of $CCR5^+CD4^+$ T cells gradually increased over time in both hNOJ (IR+) and hNOJ (IR−) mice ($n=18$ and $n=6$, respectively) (Figure 6A, left panel). Consistent with this, a substantial percentage of $CCR5^+$ cells was observed in both hNOJ (IR+) and hNOJ (IR−) mice ($n=18$ and $n=6$, respectively) and humans ($n=5$), depending on the differentiation status of the $CD4^+$ T cells (Figure 6B, left panel). However, clear differences between hNOJ mice and humans were observed. For example, more $CCR5^+$ cells were present within the $CD4^+$ T cell population in hNOJ mice than in humans, and the CM subset in hNOJ mice comprised 30−40% $CCR5^+$ cells, whereas in humans it comprised significantly fewer $CCR5^+$ cells (Figure 6B, left panel). In contrast to CCR5, CXCR4 expression was consistently observed on approximately 80% of $CD4^+$ T cells in both hNOJ (IR+) and hNOJ (IR−) mice ($n=18$ and $n=6$, respectively) throughout the course of the experiment (Figure 6A, right panel), although the percentage of CXCR4-expressing cells at an advanced differentiation stage tended to be slightly lower in both hNOJ (IR+) and hNOJ (IR−) mice ($n=18$ and $n=6$, respectively) (Figure 6B, right panel).

Ex vivo R5 HIV-1 Infectivity of Reconstituted $CD4^+$ T Cells

We next performed *ex vivo* experiments based on fusion assays using reconstituted $CD4^+$ T cells to examine the susceptibility to R5 HIV-1 infection. $CD4^+$ T cells were prepared from the spleens of hNOJ mice during the later phase (≥17 wk) post-transplantation ($n=4$; one hNOJ (IR+) and three hNOJ (IR−) mice) or from human PBMCs ($n=5$), and infected with R5 HIV-1 containing a Vpr/β-lactamase fusion protein (HIV-$1_{NL\text{-}AD8\text{-}D\text{-}BlaM\text{-}Vpr}$). Because of the limited number of detector channels on the flow cytometer, each $CD4^+$ T cell subset was defined as naïve ($CD45RA^+CCR7^+$), CM ($CD45RA^-CCR7^+$), or EM ($CD45RA^-CCR7^-$) in this experiment, and R5 HIV-1 fusion cells were detected within each subset (Figure 6C). In parallel with the low percentage of CCR5 expression, R5 HIV-1 fusion was rarely observed in the naïve subsets from both hNOJ mice and humans, confirming the CCR5-dependent infection of reconstituted $CD4^+$ T cells by R5 HIV-1.

As shown in Figure 6D, the CM and EM subsets from hNOJ mice contained significantly more R5 HIV-1 fusion cells than those derived from humans. When the amount of R5 HIV-1 fusion within each $CD4^+$ T cell subset was expressed as a value relative to that of the corresponding CM subset (which was set at 1), we found that the CM and EM subsets in both hNOJ mice and humans were highly susceptible to R5 HIV-1 compared with the naïve subset, indicating that the susceptibility to R5 HIV-1 among the $CD4^+$ T cell subsets was similar in hNOJ mice and humans (Figure 6E). Notably, despite the finding that the percentage of CCR5-expressing cells in the CM subset was nearly half that in the EM subsets (Figure 6B, left panel), R5 HIV-1 fused efficiently to both the CM and EM subsets (Figure 6D and 6E). This result is not surprising, as similar observations were also made in a simian immunodeficiency virus infection model [43]. Furthermore, the $CCR5^-$ CM subset expresses CCR5 mRNA and is very susceptible to R5 virus [44].

In vivo R5 HIV-1 Infection in hNOJ Mice

To investigate whether the different constitution of $CD4^+$ T cell subsets, i.e., naïve- or memory subset-rich, affected HIV-1 infectivity *in vivo*, we used hNOJ (IR+) mice at 10 wk post-transplantation ($n=7$) as the naïve-rich group and hNOJ (IR−) mice at ≥12 wk post-transplantation ($n=8$) as the memory-rich group. After the hNOJ mice were challenged intravenously with R5 HIV-1 (HIV-$1_{NL\text{-}AD8\text{-}D}$), the plasma viral load was monitored weekly by quantitative real-time RT-PCR up until 5 wk post-challenge.

Viral RNA was detected in the plasma of all naïve-rich hNOJ (IR+) mice at 1 wk post-challenge, and was maintained at around 1×10^5 copies/ml over time (Figure 7A, left panel). On the other hand, memory-rich hNOJ (IR−) mice showed a blunted plasma viral load during the early phase post-challenge; however, the viral load reached peak values that were approximately 1-log higher than those in naïve-rich hNOJ (IR+) mice by 5 wk post-challenge (Figure 7A, right panel). Of note, the viral load was undetectable in the plasma of two (G122-2 and G122-5) of the eight memory-rich hNOJ (IR−) mice by 1 and 2 wk post-challenge, respectively, and the mean value for the plasma viral load at 1 wk post-challenge in memory-rich hNOJ (IR−) mice was significantly lower than that in naïve-rich hNOJ (IR+) mice (Figure 7B). Surprisingly, when we compared the absolute number of peripheral blood $CD4^+$ T cells between naïve-rich hNOJ (IR+) and memory-rich hNOJ (IR−) mice just before challenge, we found that memory-rich hNOJ (IR−) mice had significantly more $CD4^+$ T cells (apart from for the naïve subset) than naïve-rich hNOJ (IR+) mice (Figure 7C), indicating that the absolute number of peripheral blood $CD4^+$ T cells at pre-challenge is not associated with the timing and level of the initial plasma viral load. However, the $CD4^+$ T cell constitution in memory-rich hNOJ (IR−) mice may contribute to subsequent virus replication, because the peak value for the plasma viral load during 5 wk post-challenge was significantly higher in memory-rich hNOJ (IR−) mice than in naïve-rich hNOJ (IR+) mice ($n=6$ and $n=7$, respectively; one hNOJ (IR+) and one hNOJ (IR−) mice were excluded from this analysis as the experiment was interrupted before 5 wk post-challenge) (Figure 7D).

To characterize the HIV-1-infected $CD4^+$ T cells further, three additional hNOJ (IR−) mice were analyzed at 2 wk post-challenge with R5 HIV-1 (Figure 8). HIV-1 infected cells were detected according to their expression of the fluorescent reporter, DsRed, by flow cytometry as described previously [29,45], and $CD4^+$ T

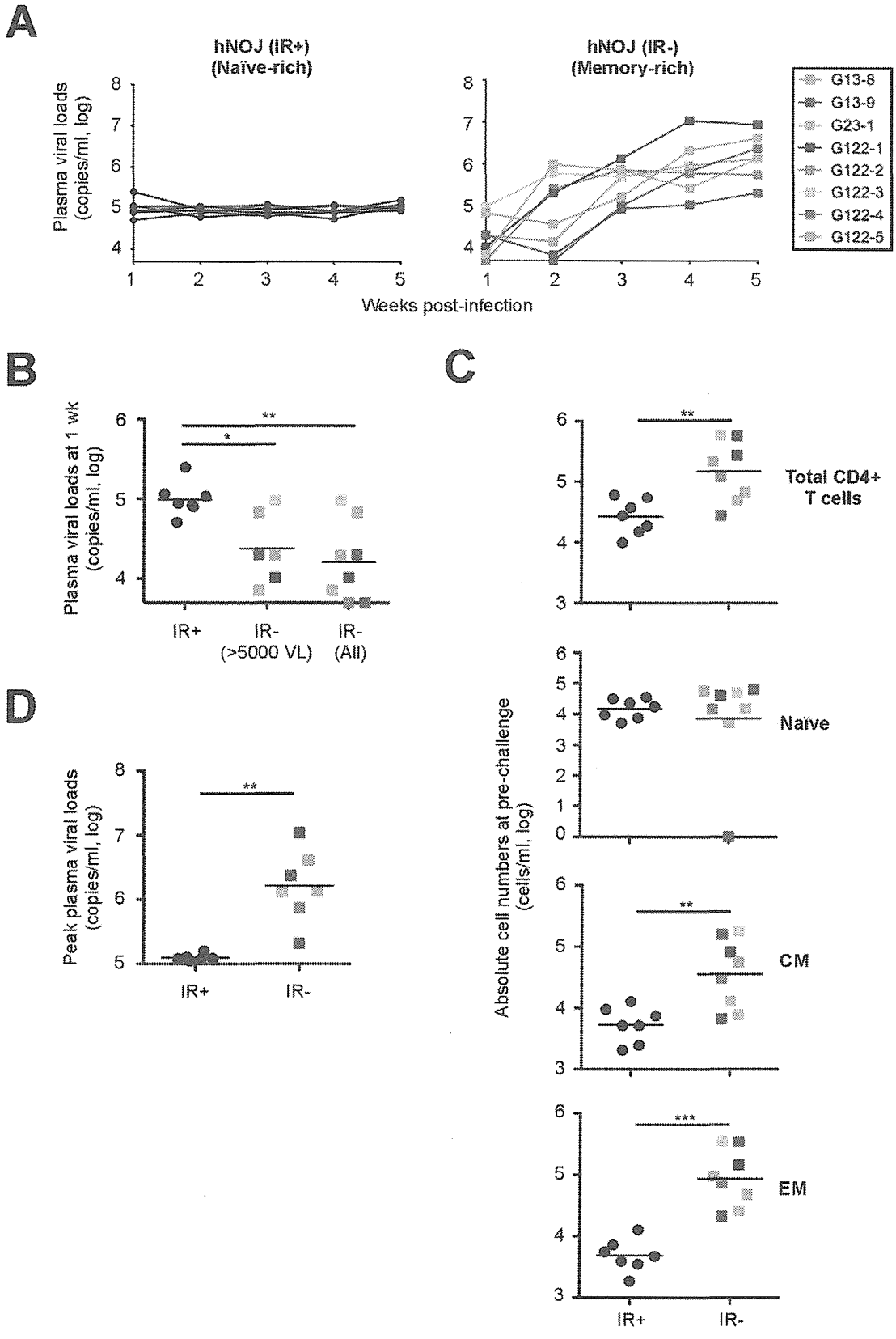

Figure 7. ***In vivo*** **R5 HIV-1 infection in hNOJ mice.** hNOJ mice were challenged intravenously with HIV-$1_{NL\text{-}AD8\text{-}D}$ and divided into two groups: naïve-rich hNOJ (IR+) mice at 10 wk post-transplantation ($n=7$) and memory-rich hNOJ (IR−) mice at ≥12 wk post-transplantation ($n=8$), based on the percentage of each individual $CD4^+$ T cell subsets at pre-challenge. (A) Weekly analysis of the plasma viral load. Individual hNOJ (IR−) mice are denoted by different colors in this and in the following figures. (B) The plasma viral load at 1 wk post-challenge. Data are plotted individually along with the mean (black lines). Significant differences ($^*P<0.05$, $^{**}P<0.01$) between hNOJ (IR+) mice ($n=7$) and hNOJ (IR−) mice in which the plasma viral

load was detectable (>5000 VL, $n=6$) or all hNOJ (IR−) mice ($n=8$) were determined by the Mann-Whitney U test. (C) The absolute number of $CD4^+$ T cells in the peripheral blood at pre-challenge [hNOJ (IR+) mice; $n=7$ and hNOJ (IR−) mice; $n=8$]. Each $CD4^+$ T cell subset (Naïve, CM, and EM) was defined as outlined in the legend to Figure 6. Data are plotted individually along with the mean (black lines). Significant differences ($^{**}P<0.01$, $^{***}P<0.001$) were determined by the Mann-Whitney U test. (D) The peak plasma viral load during 5 wk post-challenge [hNOJ (IR+) mice; $n=6$ and hNOJ (IR−) mice; $n=7$]. Data are plotted individually along with the mean (black lines). Significant differences ($^{**}P<0.01$) were determined by the Mann-Whitney U test.
doi:10.1371/journal.pone.0053495.g007

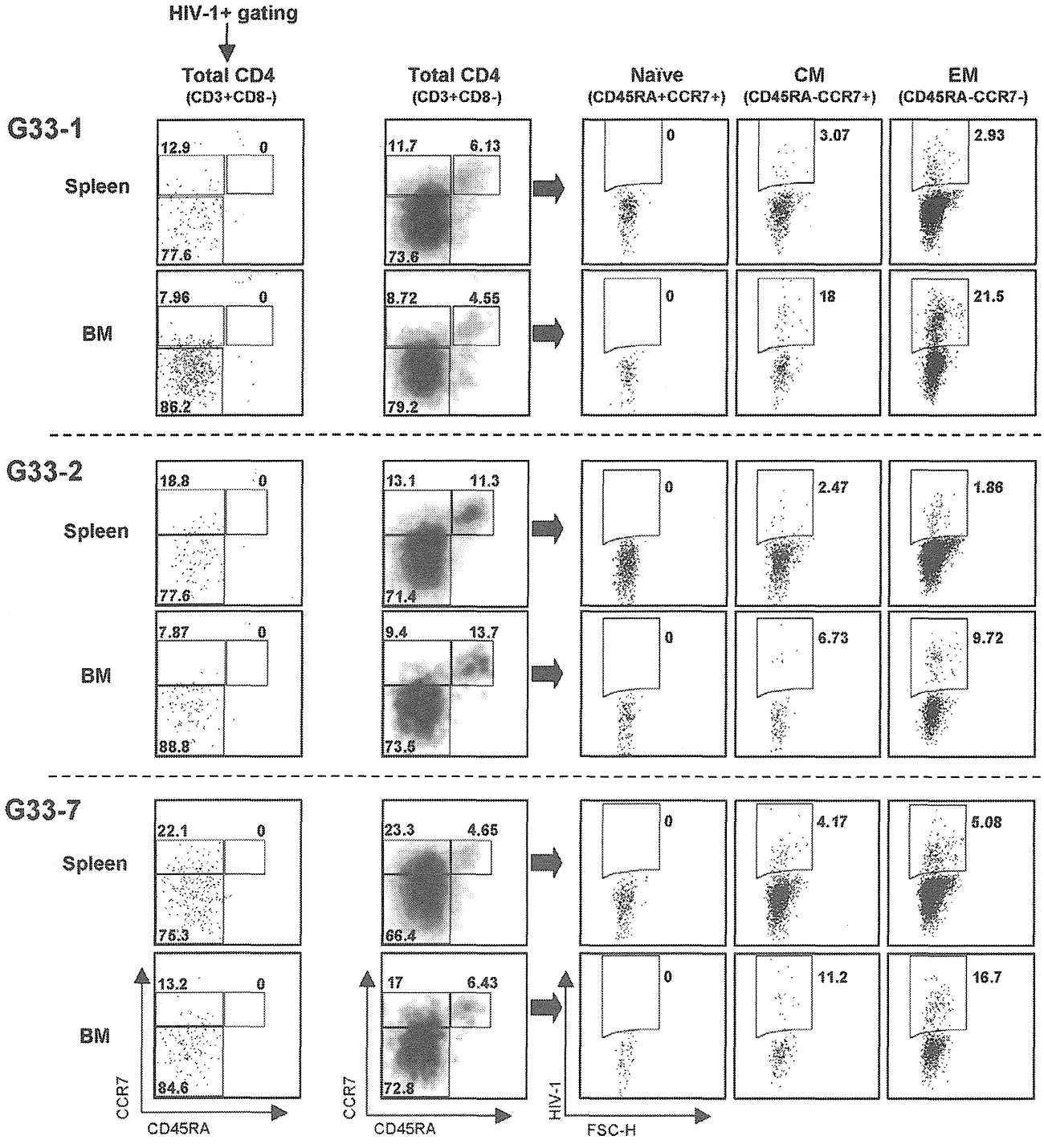

Figure 8. Identification of R5 HIV-1-infected cells in hNOJ mice. Three hNOJ (IR−) mice (G33-1, G33-2, and G33-7), all at 13 wk post-transplantation, were challenged intravenously with $HIV\text{-}1_{NL\text{-}AD8\text{-}D}$. At 2 wk post-challenge, the mice were sacrificed and the infected cells in the spleens and BM were analyzed by flow cytometry. Each $CD4^+$ T cell subset (Naïve, CM, or EM) was defined as outlined in the legend to Figure 6. Infected cells were identified based on their expression of the fluorescent reporter, DsRed.
doi:10.1371/journal.pone.0053495.g008

cells were rendered $CD3^+CD8^-$ cells in order to include CD4-downmodulated HIV-1-infected cells. When analyzing the spleens and BM, we detected infected cells within the CM and EM subsets, but not within the naïve subset. The majority of the infected cells were within the EM subset, mainly because the EM subset was the most numerous among the $CD4^+$ T cells ($CD3^+CD8^-$ cells) in both the spleens and BM at 2 wk post-challenge. However, the percentage of infected cells within the CM and EM subsets was identical. These results indicate that both the CM and EM subsets are a target of R5 HIV-1 *in vivo*.

Discussion

NOJ mice were recently developed as an alternative recipient mouse strain for the construction of humanized mice [18]. This novel strain was used in the present study. Since the Janus family tyrosine kinase, Jak3, mediates downstream signaling from the common γ chain, and is responsible for lymphocytes development [46], the phenotype of NOJ mice, which lack the *Jak3* gene, is the same as that of NOG/NSG mice [18]. Various methods are used to construct conventional humanized mouse models; however, the different methods may result in different outcomes in terms of hematopoietic cell development. Therefore, to make the experiment easier and more effective as previously suggested [9], we constructed humanized NOJ mice by transplanting $CD34^+$ HSCs isolated from umbilical cord blood into the liver of newborn mice. The present study used hNOJ mice that were not irradiated prior to HSC transplantation (i.e., hNOJ (IR−) mice), in comparison with irradiation-treated hNOJ mice (i.e., hNOJ (IR+) mice) that have been already established [18,47,48]. Each hematopoietic cell population, such as T cells, B cells, monocytes, and dendritic cells in irradiation-treated hNOJ mice show the same developmental characteristics [18,47,48] as those in other conventional humanized mouse models constructed with different strains using the same method (newborn mice were irradiated prior to intrahepatic transplantation of umbilical cord blood-derived HSCs) [16,17,49]. Therefore, hNOJ mice may be an alternative humanized mouse model, and experimental data pertaining to these hNOJ mice may be shared with other conventional humanized mouse models. However, an obvious difference between NOJ mice and other strains is their susceptibility to irradiation, which means that they have a limited life-span.

To evaluate hNOJ mice as an experimental animal model of HIV-1 infection, we first investigated how the degree of reconstitution affects the cellularity and development of $CD4^+$ T cells using hNOJ (IR+) and (IR−) mice, which represent high and low chimerism groups, respectively. However, we found that qualitative differences in the characteristics of the reconstituted $CD4^+$ T cells, such as the process of differentiation, the degree of activation, and CCR5/CXCR4 expression, were similar between hNOJ (IR+) and hNOJ (IR−) mice at least during the first 16 wk post-transplantation. In hNOJ mice, the cellularity of $CD4^+$ T cells and proportion of each $CD4^+$ T cell subset within the peripheral blood were similar to those in other organs, such as the spleen and BM (Figure 4B and data not shown), suggesting that the peripheral blood $CD4^+$ T cell population may be representative of the $CD4^+$ T cell distribution throughout other systemic compartments in these mice. In humans, the $CD45RA^+CCR7^+$ naïve and $CD45RA^-CCR7^-$ EM subsets of $CD4^+$ T cells constitute the major subset within the peripheral blood and spleen, respectively [50]. The most striking difference in the $CD4^+$ T cells between hNOJ mice and humans noted here was that hNOJ mice showed a higher percentage of $CD4^+$ T cells expressing HLA-DR, Ki-67, and CCR5 during the later phase post-transplantation.

The memory subset (either CD45RA-negative or CD45RO-positive) tends to increase with time in conventional humanized mice [28,51,52]. We found that the expansion of the $CD45RA^-CCR7^-CD27^+$ EM_{early} and $CD45RA^-CCR7^-CD27^-$ $EM_{int/late}$ subsets, but not that of the $CD45RA^-CCR7^+CD27^+$ CM subset, was associated with an activated phenotype. As suggested elsewhere [27,28], this is probably due to the occurrence of HSP, particularly HPE-type HSP, because (1) memory subsets, particularly the $EM_{int/late}$ subset, expressed the proliferation marker, Ki-67, at higher levels than the naïve subset, and the levels were much higher than those expressed by the $EM_{int/late}$ subset within human PBMC population; (2) the $EM_{int/late}$ subset showed the greatest IFN-γ-producing capacity; and (3) IL-2, IL-7, and IL-15 were undetectable in the plasma when $CD4^+$ T cells converted to an activated memory phenotype.

HPE-type HSP requires TCR-dependent antigen recognition, which is independent of IL-7 [25,26]. In line with this, Onoe *et al.* demonstrated that HPE-type HSP of $CD4^+$ T cells correlated with the percentage of $CD14^+$ monocytes in the periphery when autologous T cells reconstituted in BLT mice were adoptively transferred into T cell-deficient humanized NOD/SCID mice and suggested that $CD4^+$ T cells need to interact with self MHC-II molecules expressed by autologous myeloid-derived antigen-presenting cells (APCs) to drive their expansion [26]. Furthermore, Suzuki *et al.* used a humanized mouse model based upon HLA-DR-transgenic NOG sub-strain mice to show that expansion of the EM subset of $CD4^+$ T cells occurs in an MHC-II (HLA-DR)-dependent manner [28]. In the present study, hNOJ (IR+) mice showed a significantly higher proportion of $CD14^+$ monocytes within the PBMC population, and developed more $CD4^+$ T cells than hNOJ (IR−) mice. Although we did not examine the proportion of APCs in hNOJ (IR+) or hNOJ (IR−) mice in the present study, it is conceivable that hNOJ (IR+) mice have more APCs due to the higher level of chimerism. Therefore, TCR-dependent antigen recognition via myeloid-derived APCs may enhance HPE-type HSP of reconstituted $CD4^+$ T cells in hNOJ (IR+) mice.

The main aim of this study was to examine whether, and how, HIV-1 infectivity is affected in different humanized mouse models in which the $CD4^+$ T cell composition is qualitatively and/or quantitatively different, e.g., naïve- or memory-rich phenotypes. The results showed that the infectivity of R5 HIV-1 was different between the naïve-rich and memory-rich mouse groups. One of the most noticeable differences between the two mouse groups was that the plasma viral load at 1 wk post-challenge was significantly higher in naïve-rich hNOJ (IR+) mice than it was in memory-rich hNOJ (IR−) mice. Although robust plasma viral loads have been reported in other conventional humanized mouse models of R5 HIV-1 infection even at 1 wk post-challenge [17,53,54], our result may be curious because the R5 HIV-1 infectivity of naïve $CD4^+$ T cells is very low, and because naïve-rich hNOJ (IR+) mice would have few memory $CD4^+$ T cells compared with memory-rich hNOJ (IR−) mice. In the present study, we could not determine which cellular parameters pertaining to $CD4^+$ T cells at pre-challenge were associated with the initial plasma viral load; therefore, the reason for the difference in viral load remains unclear. One possibility may be the different proportions of dendritic cells present in hNOJ (IR+) and hNOJ (IR−) mice, since HIV-1 transmission/dissemination efficiently occurs via dendritic cell-$CD4^+$ T cell contact [3,55,56,57]. This needs to be clarified in future studies.

Another noticeable difference between naïve-rich hNOJ (IR+) and memory-rich hNOJ (IR−) mice in terms of the viral infection

was the peak level of the plasma viral load. Memory-rich hNOJ (IR−) mice showed a markedly higher peak level of the plasma viral load during 5 wk post-challenge, suggesting the contribution of the memory $CD4^+$ T cell subset in this setting. Notably, Nie *et al.* showed massive infection of the $CD45RA^-CD45RO^+CCR7^-$ EM subset by R5 HIV-1 in NOG-background humanized mice [51]. Likewise, when we analyzed the spleens and BM from hNOJ (IR−) mice at 2 wk post-challenge with R5 HIV-1, the majority of infected cells were present in the EM subset, most likely because the EM subset was the most numerous at that time. However, when individual subsets were analyzed carefully, the percentage of infected cells in the CM and EM subsets was similar. This is explained by the fact that the fusion efficiency of R5 HIV-1 was comparable between the two subsets (Figure 6E). Taken together, the data obtained in the present study suggest that the CM subset plays a role as both a target and a reservoir for R5 HIV-1 in an HIV-1 infected humanized NOJ mouse model.

hNOJ (IR+) and hNOJ (IR−) mice were highly permissive for infection with both CCR5-tropic HIV-1 (Figures 7 and 8) and CXCR4-tropic HIV-1 (data not shown). However, because hNOJ (IR+) mice have such a short life-span due to irradiation, their use is restricted to the early phase post-transplantation; their use, therefore, is restricted to the study of short-term of HIV-1 infection. By contrast, hNOJ (IR−) mice would be useful for longitudinal analyses of HIV-1 infection, as shown by other studies that used other conventional humanized mouse models [22,53,58]. However, it should be noted that level of HIV-1 infectivity would change, depending on the cellularity of the reconstituted $CD4^+$ T cells in hNOJ mice. Therefore, the selective use of humanized mice according to the disease model is important. For instance, hNOJ mice at the early phase post-transplantation would be a useful model for healthy young humans, in which the naïve $CD4^+$ T cell subset is relatively rich [59,60,61]. On the other hand, hNOJ mice at the late phase post-transplantation (i.e., hNOJ (IR−) mice), might be more suitable as a model for Immune Reconstitution Inflammatory Syndrome, which involves an activated $CD4^+$ T cell burst during post anti-retro viral therapy in HIV-infected individuals [62].

In conclusion, although no obvious differences in the cellularity of $CD4^+$ T cells were found between hNOJ (IR+) and hNOJ (IR−) mice, at least within 16 wk post-transplantation, reconstituted $CD4^+$ T cells converted to an activated memory phenotype over time. The infectivity of R5 HIV-1 was modulated *in vivo* in these humanized mice, depending on the percentage of memory $CD4^+$ T cells. Therefore, the present study suggests that humanized mouse models should be used selectively according to the experimental objectives, taking into account different human physiological states, to gain an appropriate understanding of HIV-1 infection/pathogenesis.

Acknowledgments

We thank Drs. Naoki Yamamoto and Satoru Watanabe (National University of Singapore, Singapore) for helpful advice regarding the construction of humanized mice, Dr. Minoru Tobiume (NIID, Japan) for providing pMM310, Dr. Takuya Yamamoto (National Institutes of Health, USA) for valuable discussion and Ms. Kaori Okano (our laboratory) for technical support. We also thank the Tokyo Cord Blood Bank for providing human umbilical cord blood and the Blood Bank of Japan Red Cross for providing adult human peripheral blood.

Author Contributions

Conceived and designed the experiments: KT YTY. Performed the experiments: KT MI SI YYM. Analyzed the data: KT MI SO KK YTY. Contributed reagents/materials/analysis tools: SO. Wrote the paper: KT. Edited the paper: KK YTY.

References

1. Berger EA, Murphy PM, Farber JM (1999) Chemokine receptors as HIV-1 coreceptors: roles in viral entry, tropism, and disease. Annu Rev Immunol 17: 657–700.
2. McClure MO, Sattentau QJ, Beverley PC, Hearn JP, Fitzgerald AK, et al. (1987) HIV infection of primate lymphocytes and conservation of the CD4 receptor. Nature 330: 487–489.
3. Tsunetsugu-Yokota Y (2008) Transmission of HIV from dendritic cells to $CD4^+$ T cells: a promising target for vaccination and therapeutic intervention. In: Kendow LB, editor. AIDS Vaccines, HIV Receptors and AIDS Research. New York: Nova Science Publishers, Inc. 117–128.
4. Picker LJ, Watkins DI (2005) HIV pathogenesis: the first cut is the deepest. Nat Immunol 6: 430–432.
5. Simon V, Ho DD (2003) HIV-1 dynamics in vivo: implications for therapy. Nat Rev Microbiol 1: 181–190.
6. Stevenson M (2003) HIV-1 pathogenesis. Nat Med 9: 853–860.
7. Goldstein H (2008) Summary of presentations at the NIH/NIAID New Humanized Rodent Models 2007 Workshop. AIDS Res Ther 5: 3.
8. Legrand N, Ploss A, Balling R, Becker PD, Borsotti C, et al. (2009) Humanized mice for modeling human infectious disease: challenges, progress, and outlook. Cell Host Microbe 6: 5–9.
9. Legrand N, Weijer K, Spits H (2006) Experimental models to study development and function of the human immune system in vivo. J Immunol 176: 2053–2058.
10. Manz MG (2007) Human-hemato-lymphoid-system mice: opportunities and challenges. Immunity 26: 537–541.
11. Shacklett BL (2008) Can the new humanized mouse model give HIV research a boost. PLoS Med 5: e13.
12. Sato K, Koyanagi Y (2011) The mouse is out of the bag: insights and perspectives on HIV-1-infected humanized mouse models. Exp Biol Med (Maywood).
13. Wege AK, Melkus MW, Denton PW, Estes JD, Garcia JV (2008) Functional and phenotypic characterization of the humanized BLT mouse model. Curr Top Microbiol Immunol 324: 149–165.
14. Berges BK, Rowan MR (2011) The utility of the new generation of humanized mice to study HIV-1 infection: transmission, prevention, pathogenesis, and treatment. Retrovirology 8: 65.
15. Ito R, Takahashi T, Katano I, Ito M (2012) Current advances in humanized mouse models. Cell Mol Immunol. 9: 208–214.
16. Traggiai E, Chicha L, Mazzucchelli L, Bronz L, Piffaretti JC, et al. (2004) Development of a human adaptive immune system in cord blood cell-transplanted mice. Science 304: 104–107.
17. Akkina R, Berges BK, Palmer BE, Remling L, Neff CP, et al. (2011) Humanized $Rag1^{-/-}\gamma c^{-/-}$ mice support multilineage hematopoiesis and are susceptible to HIV-1 infection via systemic and vaginal routes. PLoS One 6: e20169.
18. Okada S, Harada H, Ito T, Saito T, Suzu S (2008) Early development of human hematopoietic and acquired immune systems in new born $NOD/Scid/Jak3^{null}$ mice intrahepatic engrafted with cord blood-derived $CD34^+$ cells. Int J Hematol 88: 476–482.
19. Shultz LD, Ishikawa F, Greiner DL (2007) Humanized mice in translational biomedical research. Nat Rev Immunol 7: 118–130.
20. Liu C, Chen BJ, Deoliveira D, Sempowski GD, Chao NJ, et al. (2010) Progenitor cell dose determines the pace and completeness of engraftment in a xenograft model for cord blood transplantation. Blood 116: 5518–5527.
21. Singh M, Singh P, Gaudray G, Musumeci L, Thielen C, et al. (2012) An improved protocol for efficient engraftment in $NOD/LTSZ\text{-}SCIDIL\text{-}2R\gamma^{NULL}$ mice allows HIV replication and development of anti-HIV immune responses. PLoS One 7: e38491.
22. Watanabe S, Ohta S, Yajima M, Terashima K, Ito M, et al. (2007) Humanized $NOD/SCID/IL2R\gamma^{null}$ mice transplanted with hematopoietic stem cells under nonmyeloablative conditions show prolonged life spans and allow detailed analysis of human immunodeficiency virus type 1 pathogenesis. J Virol 81: 13259–13264.
23. Gorantla S, Sneller H, Walters L, Sharp JG, Pirruccello SJ, et al. (2007) Human immunodeficiency virus type 1 pathobiology studied in humanized BALB/c-$Rag2^{-/-}\gamma_c^{-/-}$ mice. J Virol 81: 2700–2712.
24. Boyman O, Letourneau S, Krieg C, Sprent J (2009) Homeostatic proliferation and survival of naive and memory T cells. Eur J Immunol 39: 2088–2094.
25. Min B, Yamane H, Hu-Li J, Paul WE (2005) Spontaneous and homeostatic proliferation of CD4 T cells are regulated by different mechanisms. J Immunol 174: 6039–6044.
26. Onoe T, Kalscheuer H, Chittenden M, Zhao G, Yang YG, et al. (2010) Homeostatic expansion and phenotypic conversion of human T cells depend on peripheral interactions with APCs. J Immunol 184: 6756–6765.

27. Legrand N, Cupedo T, van Lent AU, Ebeli MJ, Weijer K, et al. (2006) Transient accumulation of human mature thymocytes and regulatory T cells with CD28 superagonist in "human immune system" *Rag2*$^{-/-}\gamma_c^{-/-}$ mice. Blood 108: 238–245.
28. Suzuki M, Takahashi T, Katano I, Ito R, Ito M, et al. (2012) Induction of human humoral immune responses in a novel HLA-DR-expressing transgenic NOD/Shi-scid/γc^{null} mouse. Int Immunol 24: 243–252.
29. Yamamoto T, Tsunetsugu-Yokota Y, Mitsuki YY, Mizukoshi F, Tsuchiya T, et al. (2009) Selective transmission of R5 HIV-1 over X4 HIV-1 at the dendritic cell-T cell infectious synapse is determined by the T cell activation state. PLoS Pathog 5: e1000279.
30. Kemp K, Bruunsgaard H (2001) Identification of IFN-γ-producing CD4$^+$ T cells following PMA stimulation. J Interferon Cytokine Res 21: 503–506.
31. Cavrois M, De Noronha C, Greene WC (2002) A sensitive and specific enzyme-based assay detecting HIV-1 virion fusion in primary T lymphocytes. Nat Biotechnol 20: 1151–1154.
32. Dai J, Agosto LM, Baytop C, Yu JJ, Pace MJ, et al. (2009) Human immunodeficiency virus integrates directly into naive resting CD4$^+$ T cells but enters naive cells less efficiently than memory cells. J Virol 83: 4528–4537.
33. Tobiume M, Lineberger JE, Lundquist CA, Miller MD, Aiken C (2003) Nef does not affect the efficiency of human immunodeficiency virus type 1 fusion with target cells. J Virol 77: 10645–10650.
34. O'Doherty U, Swiggard WJ, Malim MH (2000) Human immunodeficiency virus type 1 spinoculation enhances infection through virus binding. J Virol 74: 10074–10080.
35. Saito A, Nomaguchi M, Iijima S, Kuroishi A, Yoshida T, et al. (2010) Improved capacity of a monkey-tropic HIV-1 derivative to replicate in cynomolgus monkeys with minimal modifications. Microbes Infect 13: 58–64.
36. Hiramatsu H, Nishikomori R, Heike T, Ito M, Kobayashi K, et al. (2003) Complete reconstitution of human lymphocytes from cord blood CD34$^+$ cells using the NOD/SCID/γ_c^{null} mice model. Blood 102: 873–880.
37. Yahata T, Ando K, Nakamura Y, Ueyama Y, Shimamura K, et al. (2002) Functional human T lymphocyte development from cord blood CD34$^+$ cells in nonobese diabetic/Shi-*scid*, IL-2 receptor γ null mice. J Immunol 169: 204–209.
38. Okada R, Kondo T, Matsuki F, Takata H, Takiguchi M (2008) Phenotypic classification of human CD4$^+$ T cell subsets and their differentiation. Int Immunol 20: 1189–1199.
39. Seder RA, Darrah PA, Roederer M (2008) T-cell quality in memory and protection: implications for vaccine design. Nat Rev Immunol 8: 247–258.
40. Yue FY, Kovacs CM, Dimayuga RC, Parks P, Ostrowski MA (2004) HIV-1-specific memory CD4$^+$ T cells are phenotypically less mature than cytomegalovirus-specific memory CD4$^+$ T cells. J Immunol 172: 2476–2486.
41. Chomont N, El-Far M, Ancuta P, Trautmann L, Procopio FA, et al. (2009) HIV reservoir size and persistence are driven by T cell survival and homeostatic proliferation. Nat Med 15: 893–900.
42. Surh CD, Sprent J (2008) Homeostasis of naive and memory T cells. Immunity 29: 848–862.
43. Okoye A, Meier-Schellersheim M, Brenchley JM, Hagen SI, Walker JM, et al. (2007) Progressive CD4$^+$ central memory T cell decline results in CD4$^+$ effector memory insufficiency and overt disease in chronic SIV infection. J Exp Med 204: 2171–2185.
44. Mattapallil JJ, Douek DC, Hill B, Nishimura Y, Martin M, et al. (2005) Massive infection and loss of memory CD4$^+$ T cells in multiple tissues during acute SIV infection. Nature 434: 1093–1097.
45. Terahara K, Yamamoto T, Mitsuki YY, Shibusawa K, Ishige M, et al. (2012) Fluorescent Reporter Signals, EGFP, and DsRed, Encoded in HIV-1 Facilitate the Detection of Productively Infected Cells and Cell-Associated Viral Replication Levels. Front Microbiol 2: 280.
46. Park SY, Saijo K, Takahashi T, Osawa M, Arase H, et al. (1995) Developmental defects of lymphoid cells in Jak3 kinase-deficient mice. Immunity 3: 771–782.
47. Sato Y, Takata H, Kobayashi N, Nagata S, Nakagata N, et al. (2010) Failure of effector function of human CD8$^+$ T Cells in NOD/SCID/JAK3$^{-/-}$ immunodeficient mice transplanted with human CD34$^+$ hematopoietic stem cells. PLoS One 5: e13109.
48. Sato Y, Nagata S, Takiguchi M (2012) Effective elicitation of human effector CD8$^+$ T cells in HLA-B*51:01 transgenic humanized mice after infection with HIV-1. PLoS One 7: e42776.
49. Baenziger S, Tussiwand R, Schlaepfer E, Mazzucchelli L, Heikenwalder M, et al. (2006) Disseminated and sustained HIV infection in CD34$^+$ cord blood cell-transplanted Rag2$^{-/-}\gamma_c^{-/-}$ mice. Proc Natl Acad Sci U S A 103: 15951–15956.
50. Langeveld M, Gamadia LE, ten Berge IJ (2006) T-lymphocyte subset distribution in human spleen. Eur J Clin Invest 36: 250–256.
51. Nie C, Sato K, Misawa N, Kitayama H, Fujino H, et al. (2009) Selective infection of CD4$^+$ effector memory T lymphocytes leads to preferential depletion of memory T lymphocytes in R5 HIV-1-infected humanized NOD/SCID/IL-2Rγ^{null} mice. Virology 394: 64–72.
52. André MC, Erbacher A, Gille C, Schmauke V, Goecke B, et al. (2010) Long-term human CD34$^+$ stem cell-engrafted nonobese diabetic/SCID/IL-2Rγ^{null} mice show impaired CD8$^+$ T cell maintenance and a functional arrest of immature NK cells. J Immunol 185: 2710–2720.
53. Berges BK, Akkina SR, Remling L, Akkina R (2010) Humanized Rag2$^{-/-}\gamma c^{-/-}$ (RAG-hu) mice can sustain long-term chronic HIV-1 infection lasting more than a year. Virology 397: 100–103.
54. Zhang L, Kovalev GI, Su L (2007) HIV-1 infection and pathogenesis in a novel humanized mouse model. Blood 109: 2978–2981.
55. Tsunetsugu-Yokota Y, Yasuda S, Sugimoto A, Yagi T, Azuma M, et al. (1997) Efficient virus transmission from dendritic cells to CD4$^+$ T cells in response to antigen depends on close contact through adhesion molecules. Virology 239: 259–268.
56. David SA, Smith MS, Lopez GJ, Adany I, Mukherjee S, et al. (2001) Selective transmission of R5-tropic HIV type 1 from dendritic cells to resting CD4$^+$ T cells. AIDS Res Hum Retroviruses 17: 59–68.
57. Granelli-Piperno A, Delgado E, Finkel V, Paxton W, Steinman RM (1998) Immature dendritic cells selectively replicate macrophagetropic (M-tropic) human immunodeficiency virus type 1, while mature cells efficiently transmit both M- and T-tropic virus to T cells. J Virol 72: 2733–2737.
58. Nischang M, Sutmuller R, Gers-Huber G, Audige A, Li D, et al. (2012) Humanized mice recapitulate key features of HIV-1 infection: a novel concept using long-acting anti-retroviral drugs for treating HIV-1. PLoS One 7: e38853.
59. Ponnappan S, Ponnappan U (2011) Aging and immune function: molecular mechanisms to interventions. Antioxid Redox Signal 14: 1551–1585.
60. Goronzy JJ, Lee WW, Weyand CM (2007) Aging and T-cell diversity. Exp Gerontol 42: 400–406.
61. Woodland DL, Blackman MA (2006) Immunity and age: living in the past? Trends Immunol 27: 303–307.
62. Lipman M, Breen R (2006) Immune reconstitution inflammatory syndrome in HIV. Curr Opin Infect Dis 19: 20–25.